Inverse photoemission from V, Cr, Mn, Fe, and Co monolayers on Ag(100)

J. E. Ortega and F. J. Himpsel
IBM Research Division, Thomas J. Watson Research Center, P.O. Box 218, Yorktown Heights, New York 10598
(Received 3 February 1993)

Well ordered 1×1 monolayers of transition metals are grown on Ag(100) at 440 K. Using inverse photoemission we obtain the position of the unoccupied $3d$ states versus band filling. At $k^{\parallel}=0$ the minority-spin state of Δ_5 symmetry ($d_{xz,yz}$) is found at 2.1, 1.6, 1.4, 0.5, and 0.25 eV above the Fermi level for V, Cr, Mn, Fe, and Co monolayers. For V a majority-spin feature is observed at 0.7 eV. For the Cr monolayer we obtain a magnetic exchange splitting of 2.7 eV using previous photoemission results for the majority-spin state. This is 20 times as large as in bulk Cr, suggesting a strong enhancement of the local magnetic moment in the monolayer. Our results are consistent with first-principles calculations for the magnetic configurations with the lowest energy, i.e., antiferromagnetic V, Cr, and Mn, and ferromagnetic Fe and Co monolayers on Ag(100).

I. OVERVIEW

Enhanced magnetism in monolayers[1–23] and at surfaces[24–29] has generated considerable theoretical and experimental interest. As transition-metal atoms are diluted one expects their magnetic moments to approach the atomic limit, where all spins are aligned due to Hund's rule. In the solid the spins cannot all be parallel since Pauli's principle would require the respective spatial wave functions to be orthogonal, which is impossible when the atoms are squeezed into a crystal lattice. Most of the predictions[1–5] of enhanced monolayer magnetism have been made for a Ag(100) or Au(100) substrate. The noble-metal substrate has been chosen to minimize the interference of the overlayer-to-substrate bonding with the intralayer bonding. The (100) surface orientation promises good epitaxy because many bcc transition metals (e.g., Cr and Fe) are lattice matched with the fcc noble metals Ag and Au by a factor of $\sqrt{2}$, thereby providing a one-on-one match for the atoms at the (100) interface. Early calculations[1,2] for a monolayer of Fe on Ag(100) predicted an enhancement of the magnetic moment from $2.2\mu_B$ to $3.0\mu_B$, i.e., almost halfway to the atomic limit of $4\mu_B$. Recently, a systematic first-principles study[3] of ferromagnetic and antiferromagnetic transition-metal monolayers on Ag(100) has become available. Another surprising prediction[3] has been the conversion of V from paramagnetic to antiferromagnetic as a monolayer on Ag(100).

Experimentally, these predictions have met mixed success. Particularly the existence of long-range order in the monolayer has been controversial.[7,8] The Curie temperature decreases in thin films due to the smaller number of neighbors, and it goes to zero at about a monolayer.[30,31] Photoemission and inverse photoemission[6] gave an enhanced exchange splitting for Mn and V on Ag(111), indicating an enhanced local moment according to a correlation[32,33] between exchange splitting and local magnetic moment. However, the existence of an ordered overlayer and of large-range magnetic order is doubtful for this system. The main experimental problem has been the high surface energy of transition metals, which makes it thermodynamically unfavorable to grow a flat monolayer on a noble-metal substrate, which has low surface energy. Instead, islands are formed, and intermixing occurs at steps and other defects. This is a problem inherent to enhanced monolayer magnetism, since growth on a high surface energy substrate would affect the overlayer magnetism due to hybridization with the substrate. There has been one system, i.e., Fe on Au(100), where there is evidence for an enhanced magnetic moment from an increase in the ferromagnetic exchange splitting in photoemission[18] and inverse photoemission[19] together with the observation of ferromagnetic order.[18,20,21] The surface energy problem is solved in this case by a monolayer of Au floating as a surfactant on the growing Fe layers.[19,20] For one monolayer system, i.e., Cr on Ag(100), there has been evidence[11] for a flat, well-ordered monolayer when grown at an elevated temperature of 440 K.

We find the growth at 440 K provides well-ordered monolayers not only for Cr, but also for the other transition metals. Judging by the intensity of the image potential surface state the optimum growth occurs near the middle of the $3d$ series (Mn,Cr), in agreement with surface energy arguments.[34] By going across the $3d$ series from V to Co we are able to cover the territory from a less than half filled to a nearly filled $3d$ shell, where theory predicts[3] a transition from antiferromagnetic to ferromagnetic monolayers. Using energy-dependent inverse photoemission we are able to separate $3d$-like and s,p-like states. For all the monolayers studied we find a $3d$ state of Δ_5 symmetry ($d_{xz,yz}$) and an s,p state of Δ_1 symmetry (s,p_z) that can be viewed as the monolayer limit of a quantum-well state by analogy with results[19] from Fe/Au(100). The $3d$ state moves towards the Fermi level when increasing the atomic number from Cr to Co due to band filling. It is consistent with the position of the minority-spin state obtained in first-principles band calculations.[3] For V the d band is less than half filled, giving rise to a majority-spin feature near the Fermi level in addition to a minority state.

0163-1829/93/47(24)/16441(6)/$06.00

II. GROWTH OF FLAT MONOLAYERS

Smooth Ag(100) and Au(100) substrates were prepared by mechanical and chemical polishing and by several cycles of sputter annealing with 500 eV Ar ions at $\pm 30°$ from grazing. The details of the substrate preparation are described in Ref. 35. The clean Ag(100) surface exhibited a sharp, low-background 1×1 low-energy electron-diffraction (LEED) pattern, and the Au(100) surface exhibited 5×20 reconstruction. Both surfaces gave strong emission from image potential surface states,[35] which we found to be a good indicator of surface perfection.

Transition-metal layers were deposited from miniature electron-beam evaporators operating in the 10^{-10} range at low evaporation rates (0.5 layer/min). The evaporated layers were insensitive to the residual gases in the UHV chamber (a few days at 5×10^{-11} Torr, with mostly H_2), but the image state in the inverse photoemission spectra shifts up by 0.3 eV with 10 L O_2. The thickness was controlled with a quartz monitor, which was calibrated for different elements with medium-energy ion scattering. An additional check of the coverage calibration can be made with the image state, which commonly characterizes the top layer of the substrate, since the position of the image state is tied to the work function.

Figure 1 shows the coverage dependence of inverse photoemission spectra for Mn on Ag(100), evaporated at 300 K. The coverage-dependent image state energy is shown in the inset. It changes linearly in the submonolayer regime and stabilizes above one monolayer. The intersection point of the two asymptotes would correspond to exactly one layer coverage for ideal layer-by-layer growth. Deviations from linearity around this point are due to the presence of second-layer atoms before completion of the first layer. Another indicator of the onset of multilayer formation is the width of the 3*d* states of the transition metal. Following the Mn 3*d* feature in Fig. 1 we see a single peak in the submonolayer regime, as expected for a two-dimensional system. For thicker layers this feature broadens and splits due to three-dimensional band dispersion. Thereby it fills in states near the Fermi level, i.e., between the unoccupied minority-spin peak and its occupied majority-spin counterpart, and thus reduces the magnetic splitting (see discussion in Sec. V). The broader Mn 3*d* structure starts to develop already in the monolayer spectrum, indicating the population of several layers for a nominal coverage of one layer. This happens at room temperature, where the surface mobility is not high enough to spread out the Mn layer completely.

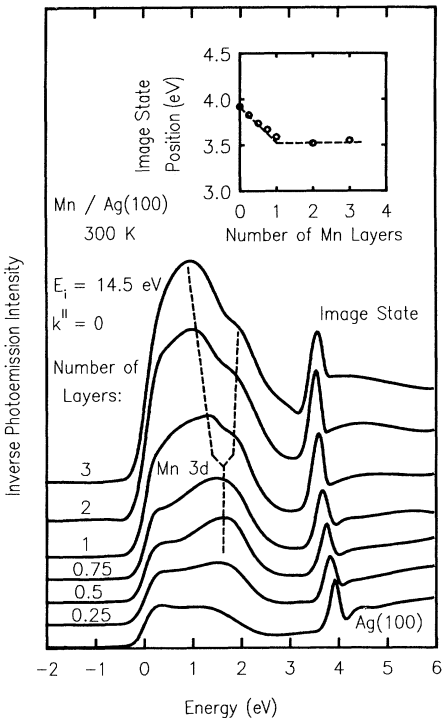

FIG. 1. Evolution of the Mn 3*d* bands with film thickness for Mn on Ag(100). Up to a monolayer a single 3*d* peak is observed, which is assigned to the minority-spin states of the local-density of states. Above one layer the 3*d* peak splits due to three-dimensional band dispersion. The position of the image state (inset) reflects the work-function change. Its saturation confirms the completion of a monolayer.

In order to improve the monolayer morphology we have raised the growth temperature, promoting surface diffusion (see Fig. 2 for a Cr monolayer). According to previous work[10,11] on the growth of Cr on Ag(100) one has to strike a delicate balance between surface ordering by diffusion and island formation as a function of the temperature. It was found by photoelectron diffraction

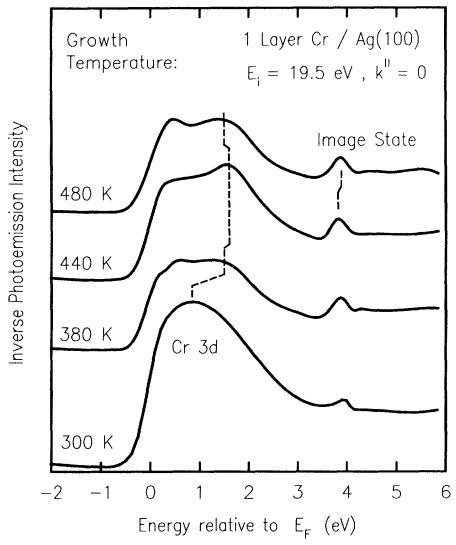

FIG. 2. Temperature dependence of the growth of a Cr monolayer on Ag(100) showing an optimum growth temperature of 440 K, in agreement with previous work (Ref. 11). The 3*d* state is sharpest and highest in energy at 440 K, thereby producing the largest magnetic splitting. At room temperature the Cr 3*d* states are shifted towards the Fermi level and broadened, indicating three-dimensional band dispersion due to multilayer growth. Above 440 K silver segregates to the surface and shifts the image state.

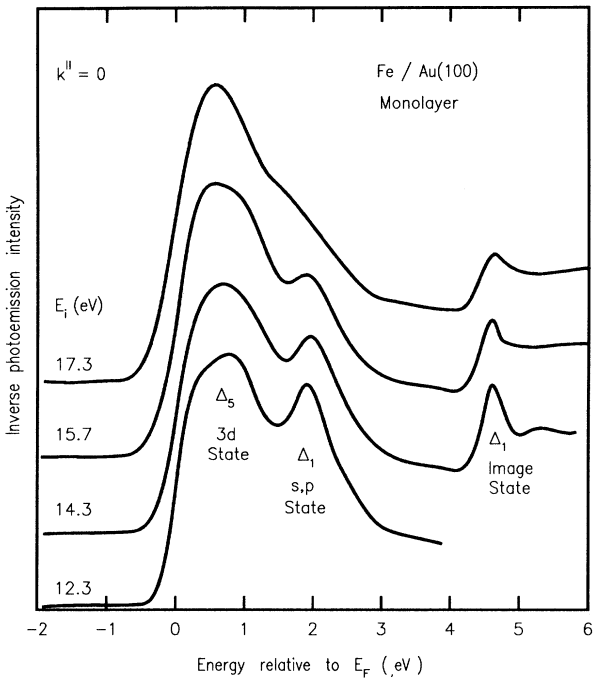

FIG. 3. Energy-dependent cross section of s,p vs $3d$ states for a Fe monolayer on Au(100). At low initial energy E_i the s,p-like states dominate, while at high E_i the $3d$ states dominate.

that high-temperature growth (500 K) leads to the formation of three-dimensional islands, while lower temperatures (300 K) produce disordered layers. Well-ordered Cr monolayers could only be grown on Ag(100) at temperatures around 440 K. Several phenomena may play a role, such as segregation of silver to the surface due to its low surface energy. Intermixing could also happen, but it is energetically unfavorable according to the bulk phase diagram. These factors naturally affect the electronic states in the inverse photoemission spectra, changing their character from two or three dimensions or changing the work function and thereby the position of the image potential surface state. In Fig. 2 we show the inverse photoemission spectra for a monolayer of Cr grown on Ag(100) at four different temperatures. The spectra have been taken at an incident energy $E_i = 19.5$ eV to enhance emission from Cr $3d$-like states (see Fig. 3 and Sec. III). The $3d$ feature is sharpest when the layer is deposited at 440 K, indicating the best growth condition for a flat, two-dimensional monolayer. Our spectroscopic data thus agree with the structural data of Ref. 11 in giving an optimum growth temperature of 440 K. At higher temperature (500 K) the image state shifts upwards and reaches the same position as for clean Ag(100). This effect can be either explained with the presence of segregated Ag in the topmost layer or with the formation of Cr islands. This observation agrees with the analysis of the Ag surface-state peak in photoemission and with photoelectron diffraction results.[10,11] At lower temperature (300 K) the Cr $3d$ states are broader, either due to disorder or due to multilayer growth. They are also closer to the Fermi level, suggesting a smaller magnetic exchange splitting and smaller magnetic moment (see Sec. V).

We have extended the search for optimum monolayer growth conditions to a large part of the $3d$ transition-metal series on Ag(100) and have found that better ordered 1×1 layers can be grown for all of them at 440 K, judging from the sharpness and position of the $3d$ states and the intensity of the image states. Although there is always an improvement by going to 440 K there remain variations in the intensity of the image states across the $3d$ series, as shown in Fig. 4. Elements with a nearly

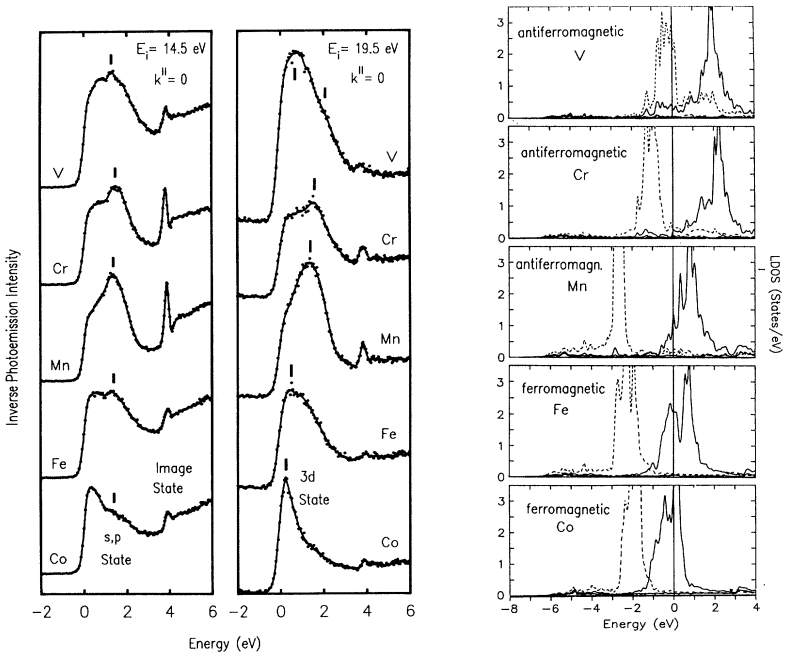

FIG. 4. Trends in the position of the s,p and $3d$ states for transition-metal monolayers on Ag(100). The s,p states (left) are nearly independent of the atomic number Z while the $3d$ states (middle) move down with increasing Z due to band filling. The densities of states calculated for the most stable monolayer configurations on Ag(100) in Ref. 3 are reproduced in the right panel (dashed lines for majority-spin states, solid lines for minority-spin states). They reflect the same trend.

half-filled $3d$ shell (Mn,Cr) exhibit the strongest image states. This observation fits in nicely with surface energy arguments. The surface energy has a minimum near the middle of the $3d$ series according to surface tension measurements and local-density calculations,[34] thus making the formation of a flat monolayer more favorable. Indeed, the intensity of the image potential state in Fig. 4 scales inversely with the surface energy reported in Ref. 34. A simple explanation for this behavior is the large magnetic splitting that separates the majority- and minority-spin states almost completely (see Secs. IV and V). For a half-filled d band the energy of the occupied, majority-spin states is lowered compared to the nonmagnetic case, and very few high-energy $3d$ states are left at the Fermi level.

For a complete surface energy balance we have to consider whether or not there is a layer of Ag segregating to the surface that reduces the surface energy. Such a phenomenon has been observed[19,20] for the growth of Fe on Au(100) at room temperature. It should become enhanced when growing at elevated temperature. In order to look for the presence of a Ag surfactant overlayer we can check the work function by the position of the image state energy. However, this analysis is inconclusive due to the small difference in energy between the image state for clean Ag(100) (3.93 eV) and that for the transition metals [e.g., 3.7 eV (Ref. 36) for Fe(100)]. In the spectra of Fig. 4 the image states are located at 3.87, 3.84, 3.89, 3.94, and 3.92 eV for a monolayer of V, Cr, Mn, Fe, and Co, respectively. In the case of Cr on Ag(100) it has been found by photoelectron diffraction[11] that the emission from the Cr layer was isotropic, and did not exhibit the forward diffraction maxima expected from an ordered Ag(100) surfactant overlayer. A possibility that cannot be reluctant is some alloying of Ag within the transition-metal monolayer, without extra Ag atoms on top.

III. INVERSE PHOTOEMISSION RESULTS

The experiments were performed with a tunable inverse photoemission system described previously.[37] The energy resolution has been improved[36] to better than 0.26 eV (photons plus electrons) at the lowest incident energy used here (14.5 eV). All data were taken at normal incidence of the electrons ($k^{\parallel}=0$) with a detection probability three times higher for photons polarized with the electric-field vector normal to the surface than parallel. Dipole selection rules allow transitions into states of Δ_1 (s,p_z,d_z^2) and Δ_5 ($p_{xy},d_{xz,yz}$) symmetry, with Δ_5 having three times more weight under the given polarization conditions.

The tunability of our photon detector allows us to separate d-like states from s,p states by their energy-dependent cross sections. This can be seen best from data with a Au(100) substrate (Fig. 3), where a very flat monolayer can be grown since the gold floats on top of the Fe layer as surfactant.[19,20] In this case one can clearly separate a Δ_5 $3d$ state and a Δ_1 s,p state. They connect with the corresponding bulk states of Fe(100) when going to thicker films (see Ref. 19). The $3d$ state becomes stronger at higher initial energies E_i, and the s,p state becomes weaker. Figure 4 shows similar inverse photoemission spectra for monolayers of transition metals on Ag(100), taken with two different initial energies of 14.5 and 19.5 eV to emphasize the s,p and $3d$ states, respectively. The features are assigned according to their energy-dependent intensity (see tick marks in Fig. 4) and their respective energies are plotted in Fig. 5. Since these are two-dimensional states there is no band dispersion when changing the initial energy. This can be seen in the Fe/Au(100) spectra in Fig. 3 and appears also to hold for the less-resolved spectra on Ag(100) in Fig. 4.

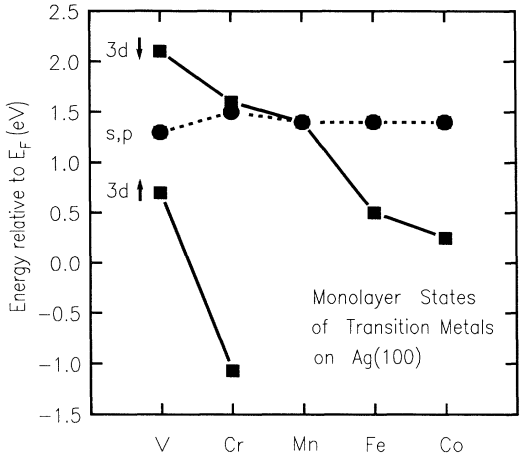

FIG. 5. Energy positions of the states shown in Fig. 4 together with photoemission results for Cr from Ref. 10. The magnetic exchange splitting of 2.7 eV for the Cr monolayer on Ag(100) is much larger than that of 0.13 eV (Ref. 40) for bulk Cr, demonstrating strongly enhanced local moments in the monolayer.

IV. COMPARISON WITH LOCAL-DENSITY THEORY

First-principles, local-density band calculations have been performed for a number of transition-metal monolayers on the (100) surface of noble metals.[1–5] Recently, a systematic study[3] of monolayers on Ag(100) has been carried out across the whole transition-metal series. By minimizing the total energy it has been found that elements with a nearly filled $3d$ shell prefer to be ferromagnetic (Fe,Co,Ni), while elements with roughly half filled $3d$ sell prefer to order antiferromagnetically in checkerboard fashion (V,Cr,Mn). The density of states calculated for the lowest-energy configurations is compared to our inverse photoemission data in Fig. 4. It should be noted that there is no strict correspondence between data and theory in Fig. 4 since the data are momentum resolved ($k^{\parallel}=0$) and symmetry resolved (Δ_5 symmetry for the $3d$ feature), while the calculated density of states in-

tegrates over the band dispersion parallel to the surface and over all symmetries. Nevertheless, a comparison makes sense since the calculated band dispersion is small compared to the magnetic splitting, which separates the density of states into a minority- and majority-spin peak. This is due to the weakened coupling of the transition-metal atoms in the monolayer, which reduces the bandwidth and increases the magnetic splitting. This is the very effect that causes enhanced magnetism. Therefore, we use the qualitative features of the calculated density of states to assign our features. For Cr, Mn, Fe, and Co the majority-spin band is almost completely occupied, such that we only see the minority band with inverse photoemission. For V the majority-spin peak starts to cross the Fermi level, giving rise to a new, low-energy peak in the inverse photoemission spectrum, while the minority-spin feature persists as a weak shoulder on the high-energy side of the majority peak. Since the actual magnetic order of these monolayers has not yet been determined experimentally, it is understood that we are talking about the local spin density at a given atomic site, irrespective of long-range order. Long-range, ferromagnetic order has been established so far only for a monolayer of Fe on Au(100), in agreement with theory. The position of the experimental minority-spin $3d$ feature shifts down with increasing atomic number Z, due to d-band filling. It is 2.1, 1.6, 1.4, 0.5, and 0.25 eV for V, Cr, Mn, Fe, and Co. This compares to calculated values of 1.9, 2.2, 0.8, 0.8, and 0.1 eV for antiferromagnetic V, Cr, and Mn, and ferromagnetic Fe and Co. The majority peak in V lies at 0.7 eV, but it is cut off by the Fermi level and consistent with a density-of-states maximum below the Fermi level, as predicted in the calculation (-0.3 eV). The general filling trend towards lower energies at higher atomic number is found in both the calculation and the experiment. Discrepancies generally are comparable to the experimental and calculated peak widths.

The experimental s,p states are not easily compared with the calculation, since they give rise to a relatively low density of states, which is lost under the strong $3d$ peaks in the total density of states. The fact that the s,p state does not shift much across the transition-metal series is analogous to the three-dimensional case, where the bulk s,p band remain almost stationary, while the $3d$ band shifts to take up the extra electrons (see Ref. 38). Another way of looking at the s,p-like states is provided by a quantum-well picture.[19,39] In a thin film one expects a quantization of the bulk s,p states in the direction perpendicular to the surface, leading to a set of discrete states instead of a continuum. Their number decreases when the number of atomic layers in the film is reduced. In the monolayer limit there is only a single quantum-well state left. Due to the particular boundary conditions at the Ag(100) surface this state persists even in the zero coverage limit and approaches an intrinsic surface resonance of Ag(100), which represents the $n=0$ extrapolation of the image potential state series (see Refs. 35 and 39 for details). The $n=0$ resonance has been found[35] at 1.3 eV for Ag(100), and can be seen as a shoulder in the bottom spectrum of Fig. 1. Since all the monolayer states approach the same substrate surface resonance they have a similar energy (about 1.4 eV), nearly independent of the transition metal.

V. MAGNETIC EXCHANGE SPLITTING AND MOMENT

A key property of the monolayer electronic structure is the magnetic exchange splitting between majority- and minority-spin states. We can infer the local magnetic moment from it, including its predicted enhancement, by using a correlation of about 1 eV/μ_{Bohr}, between the magnetic $3d$ splitting and the local magnetic moment. This relation holds empirically for a large variety of magnetic systems[32] and has recently been confirmed by local-density calculations[33] for a variety of alloys. The magnetic exchange splitting is accessible for some of the transition-metal monolayers studied here. For the Cr monolayer, the majority-spin counterpart to our Δ_5 state has been found at -1.07 eV in photoemission experiments.[10] This allows us to determine an exchange splitting of 2.7 eV for this state. A similar value of 2.5–2.6 eV has been found[14] for a Cr monolayer on Au(100). The calculated average splitting between the two peaks in the density of states (see Fig. 4 and Ref. 3) is 3.3 eV, with a calculated magnetic moment of $3.7\mu_{\text{Bohr}}$. All of these values are clearly much larger than the magnetic splitting[40] of 0.13 eV in antiferromagnetic bulk Cr. Monolayers of Cr thus provide the largest effect observed so far in the enhancement of magnetism at surfaces, i.e., about a factor of 20. This is in agreement with the expectation that the local magnetic moment should be maximized for a half filled shell, where Hund's rule lines up all the spins in the dilute limit. For the V monolayer on Ag(100) we can obtain a lower limit of 1.4 eV for the magnetic exchange splitting from our inverse photoemission data. The actual value might be larger due to majority-spin states below the Fermi level. This compared with a momentum-averaged splitting of 2.2 eV and a magnetic moment of $2.1\mu_{\text{Bohr}}$ in the calculation.[3] Since bulk V is paramagnetic we have again a large enhancement of the local magnetic moment, but the existence of long-range order in this system remains controversial.[7,8] Likewise, long-range antiferromagnetic order has not yet been clearly established for the Cr monolayer on Ag(100), although a weak $c(2\times2)$ LEED pattern has been taken as an indication of antiferromagnetic ordering.[10]

Our results can be compared with previous data from transition-metal monolayers on noble metals. There exists early inverse photoemission work[6] on Mn and V monolayers on Ag(111), which already indicated a large magnetic exchange splitting and hence a large local magnetic moment. On the (111) surface, however, the structure of the transition-metal layers is complicated since there is no lattice match, and a comparison with theory is not possible. Results[18,19] for a ferromagnetic monolayer of Fe on Au(100) gave a 40% enhancement of the magnetic splitting for the same Δ_5 state that we observe on Ag(100), but only a marginal change for the $3d$-like Δ_1 states [not to be confused with the s,p-like Δ_1 states discussed here on Ag(100)].

In summary, our systematic study of the position and

magnetic splitting of 3*d* states in transition-metal monolayers on Ag(100) gives strong evidence of enhanced monolayer magnetism as a general phenomenon. However, we can state this result only on a local scale. An unambiguous determination of the long-range magnetic order is still outstanding for most of these systems.

ACKNOWLEDGMENT

We would like to acknowledge M. Copel for Rutherford backscattering experiments that were used for our thickness calibration.

[1]C. L. Fu, A. J. Freeman, and T. Oguchi, Phys. Rev. Lett. **54**, 2700 (1985); S. Ohnishi, C. L. Fu, and A. J. Freeman, J. Magn. Mater. **50**, 161 (1985); A. J. Freeman and C. L. Fu, J. Appl. Phys. **61**, 3356 (1987); Chun Li, A. J. Freeman, and C. L. Fu, J. Magn. Magn. Mater. **75**, 201 (1988); Chun Li, A. J. Freeman, H. J. F. Jansen, and C. L. Fu, Phys. Rev. B **42**, 5433 (1990); A. J. Freeman and Ru-qian Wu, J. Magn. Magn. Mater. **100**, 497 (1991).

[2]Roy. Richter, J. G. Gay, and John R. Smith, Phys. Rev. Lett. **54**, 2704 (1985).

[3]S. Blügel, M. Weinert, and P. H. Dederichs, Phys. Rev. Lett. **60**, 1077 (1988); S. Blügel, B. Drittler, R. Zeller, and P. H. Dederichs, Appl. Phys. A **49**, 547 (1989); S. Blügel, Phys. Rev. Lett. **68**, 851 (1992).

[4]Ming J. Zhu, D. M. Bylander, and L. Kleinman, Phys. Rev. B **43**, 4007 (1991).

[5]Olle Eriksson, R. C. Albers, and A. M. Boring, Phys. Rev. Lett. **66**, 1350 (1991).

[6]W. Drube and F. J. Himpsel, Phys. Rev. B **35**, 4131 (1987).

[7]C. Rau, G. Xing, and M. Robert, J. Vac. Sci. Technol. A **6**, 579 (1988); C. Rau, G. Xing, C. Liu, and M. Robert, Phys. Lett. **135**, 227 (1989); C. Rau, Appl. Phys. A **49**, 579 (1989).

[8]M. Stampanoni, A. Vaterlaus, D. Pescia, M. Aeschlimann, F. Meier, W. Dürr, and S. Blügel, Phys. Rev. B **37**, 10 380 (1988); R. L. Fink, C. A. Ballentine, J. L. Erskine, and Jose A. Araya-Pochet, *ibid.* **41**, 10 175 (1990).

[9]D. A. Newstead, C. Norris, C. Binns, and P. C. Stephenson, J. Phys. C **20**, 6245 (1987).

[10]C. Krembel, M. C. Hanf, J. C. Peruchetti, D. Bolmont, and G. Gewinner, Phys. Rev. B **44**, 11 472 (1991).

[11]C. Krembel, M. C. Hanf, J. C. Peruchetti, D. Bolmont, and G. Gewinner, Phys. Rev. B **44**, 8047 (1991); Surf. Sci. **269/270**, 748 (1992); J. Vac. Sci. Technol. A **10**, 3325 (1992).

[12]M. C. Hanf, C. Pirri, J. C. Peruchetti, D. Bolmont, and G. Gewinner, Phys. Rev. B **36**, 4487 (1987); **39**, 1546 (1989).

[13]D. G. O'Neill and J. H. Weaver, Phys. Rev. B **37**, 8122 (1988).

[14]M. E. Haugan, Qibiao Chen, M. Onellion, and F. J. Himpsel (unpublished).

[15]B. T. Jonker, K.-H. Walker, E. Kisker, G. A. Prinz, and C. Carbone, Phys. Rev. Lett. **57**, 142 (1986).

[16]N. C. Koon, B. T. Jonker, F. A. Volkening, J. J. Krebs, and G. A. Prinz, Phys. Rev. Lett. **59**, 2463 (1987).

[17]C. J. Gutierrez, S. H. Mayer, and J. C. Walker, J. Magn. Magn. Mater. **80**, 299 (1989).

[18]W. Heinen, C. Carbone, T. Kachel, and W. Gudat, J. Electron Spectrosc. Relat. Phenom. **51**, 701 (1990).

[19]F. J. Himpsel, Phys. Rev. B **44**, 5966 (1991).

[20]S. D. Bader, E. R. Moog, and P. Grünberg, J. Magn. Magn. Mater. **53**, L295 (1986); S. C. Bader and E. R. Moog, J. Appl. Phys. **61**, 3729 (1987); C. Liu and S. D. Bader, J. Vac. Sci. Technol. A **8**, 2727 (1990).

[21]W. Dürr, M. Taborelli, O. Paul, R. Germar, W. Gudat, D. Pescia, and M. Landolt, Phys. Rev. Lett. **62**, 206 (1989).

[22]H. J. Elmers, G. Liu, and U. Gradmann, Phys. Rev. Lett. **63**, 566 (1989).

[23]H. Li, S. C. Wu, D. Tian, Y. S. Li, J. Quinn, and F. Jona, Phys. Rev. B **44**, 1438 (1991).

[24]G. Allan, Phys. Rev. B **19**, 4774 (1979).

[25]S. Bouarab, H. Nait-Laziz, C. Demangeat, A. Mokrani, and H. Dreysse, J. Magn. Magn. Mater. **102**, L233 (1991).

[26]S. Ohnishi, A. J. Freeman, and M. Weinert, Phys. Rev. B **28**, 6741 (1983).

[27]C. Rau, C. Liu, A. Schmalzbauer, and G. Xing, Phys. Rev. Lett. **57**, 2311 (1986).

[28]L. E. Klebanoff, R. H. Victora, L. M. Falicov, and D. A. Shirley, Phys. Rev. B **32**, 1997 (1985).

[29]D. Weller, S. F. Alvarado, W. Gudat, K. Schröder, and M. Campagna, Phys. Rev. Lett. **54**, 1555 (1985).

[30]Z. Q. Qiu, J. Pearson, and S. D. Bader, Phys. Rev. Lett. **67**, 1646 (1991).

[31]G. J. Mankey, M. T. Kief, and R. F. Willis, J. Vac. Sci. Technol. A **9**, 1595 (1991); F. Huang, G. J. Mankey, M. T. Kief, and R. F. Willis, J. Appl. Phys. (to be published).

[32]F. J. Himpsel, Phys. Rev. Lett. **67**, 2363 (1991); J. Magn. Magn. Mater. **102**, 261 (1991).

[33]I. Turek, Ch. Becker, and J. Hafner, J. Phys. Condens. Matter **4**, 7257 (1992).

[34]M. Aldén, H. L. Skriver, S. Mirbt, and B. Johansson, Phys. Rev. Lett. **69**, 2296 (1992).

[35]F. J. Himpsel and J. E. Ortega, Phys. Rev. B **46**, 9719 (1992).

[36]F. J. Himpsel, Phys. Rev. B **43**, 13 394 (1991).

[37]Th. Fauster, D. Straub, J. J. Donelon, D. Grimm, A. Marx, and F. J. Himpsel, Rev. Sci. Instrum. **56**, 1212 (1985).

[38]F. J. Himpsel, Adv. Phys. **32**, 1 (1983), see Fig. 19.

[39]J. E. Ortega and F. J. Himpsel, Phys. Rev. Lett. **69**, 844 (1992); J. E. Ortega, F. J. Himpsel, G. J. Mankey, and R. F. Willis, Phys. Rev. B **47**, 1540 (1993).

[40]L. W. Bos and D. W. Lynch, Phys. Rev. B **2**, 4567 (1970).